Modelling intertidal area evolution in the Western Scheldt

Hindcast (1964-2010) and
forecast (2020-2100) under sea level rise scenarios

Modelling intertidal area evolution in the Western Scheldt
Hindcast (1964-2010) and forecast (2020-2100) under sea level rise scenarios

Client	Rijkswaterstaat-
Contact	Marco Schrijver, Gert-Jan Liek
Reference	
Keywords	Western Scheldt, intertidal area, sea level rise

Document control	
Version	1.0
Date	11-03-2025
Project nr.	11210344-001
Document ID	11210344-001-ZKS-0002
Pages	38
Classification	
Status	final

Author(s)

	Mick van der Wegen	
	Mónica Aguilera Chaves	

Summary

The Western Scheldt comprises about 92 km^2 of intertidal areas, including sandy and muddy shoals and large marsh regions like the Land van Saeftinghe. Some areas are attached to the estuary's shorelines, while others are surrounded by channels. These intertidal zones hold significant ecological value and contribute to flood protection through wave attenuation. Over time, the intertidal area slowly evolves in size and height due to tidal and wave forces, as well as human interventions such as dredging and disposal activities. Measurements indicate a 2% decrease in intertidal area and a 30% increase in mean intertidal area height from 1965 to 2010.

This study aims to assess the performance of process-based morphodynamic modelling (Delft3D) in predicting the evolution of intertidal flats in the Western Scheldt and to explore the potential impacts of sea level rise (SLR) and dredge-disposal strategies. The analysis focuses on morphodynamic hindcast results between 1965 and 2010 and forecast results from 2020-2100, examining intertidal area evolution in terms of general patterns, hypsometry, area and mean height. The Delft3D model is 2D, includes one, 200 µm sand fraction, dredging/disposal activities and a schematized, one-direction wind/wave field.

During the hindcast period, the model's deviations from observations are in the same order of magnitude as the observed changes (~10% of the actually observed intertidal area and mean height). This indicates challenges in accurately reproducing observed variations. Initially, the model underestimated the increase in intertidal area and later overestimated the decrease. In the first decades, the model underestimated the increase in mean height, but the error became negligible after 45 years. Adding waves sometimes improved the model performance and sometimes not. Model performance was generally worse when subregions were analysed, suggesting that regional differences in model performance partly average out in the total area analysis.

The 80-year model forecast shows a clear declining trend in intertidal area under various scenarios with 3m/century SLR (-20 to -40%), while no-SLR scenarios maintain more intertidal area (-5 to +20%). Model deviations found in the hindcast (max 10% of the present area and height) remain lower than the extreme SLR impact. Intermediate SLR scenarios interpolate between these extremes. Model results indicate that a strategy disposing more sediments in the eastern part and deeper parts of the main channel leads to about 10% more intertidal area loss compared to a strategy disposing sediments near intertidal areas throughout the estuary.

Our analysis suggests that process-based modelling has potential in predicting long-term (>decadal) trends of intertidal flat evolution, especially when considering larger-scale interventions and long-term changes in forcing (SLR, dredging and disposal strategies). To improve model performance, future work may include 3D dynamics, mud, and more advanced schematizations of the wave field and dredging/disposal algorithms. Comparison results to other modelling efforts (ASMITA/ESTMORF/Delft3D hybrid) may enhance confidence in model predictions under SLR scenarios.

Contents

1 Introduction

Within the VNSC framework to assess the long-term perspective of Western Scheldt morphodynamics and hydrodynamics, this report focuses on the long-term evolution of Western Scheldt intertidal area. Intertidal area is important in relation to future nature values in the Western Scheldt, but it also plays an important role in tidal asymmetry, associated sediment transports and sediment budgets. Appendix A includes a figure including the morphological components of the Western Scheldt. Past studies (e.g De Vet et al., 2017) have focussed on an analysis of historic bathymetric data, but morphodynamic forecast studies remain quite limited.

The objective of this report is to assess the Röbke et al. (2020) Delft3D model results in terms of intertidal area including a 1965-2010 hindcast and a 2020-2100 forecast under scenarios of sea level rise and dredging. A major part of the results presented in this report is based on an improved analysis of the bachelor thesis research carried out in spring 2024 at Deltares (Paternotte, 2024).

Our analysis shows the potential value of process-based models in predicting the morphodynamic evolution of intertidal flats under sea level rise and scenarios of human interventions. These insights are important to assess the value of applying process-based modelling tools in planning integral sediment management strategies.

2 Method

2.1 Summary of numerical model set-up and scenarios

Röbke et al. (2020) provide a detailed description of the computational grid, set-up, calibration and validation of the model. Sensitivity runs and scenarios included different SLR rates, inclusion/exclusion of a unidirectional “representative” wind/wave field, dredge and disposal scenarios and inclusion or exclusion of nourishments in the mouth area. Table 1 provides an overview of runs analysed in this report. Even though in the original study by Röbke et al. (2020), the hindcast period was 1964-2012, the hindcast simulations were re-analyzed for the period 1965-2010. This way, the starting point for comparison with available measurements was the same. The hindcast DAD (Dredging And Disposal) algorithm maintains a prescribed minimal depth at every timestep in the polygon-defined area of the main access channel. The minimum depth is time dependent following changing access channel depth requirements over the 45 year period. The disposal areas were kept constant according to the 2013-14 conditions. Sand mining is based on the average yearly sand mining volumes in the period 1963-2012 (i.e. 2410100 m^3/yr). This yearly volume is divided by the number of sand mining polygons (33) and then used as a constant sand mining volume of about 73000 m^3 per polygon.

All forecast runs are preceded by a 25 year morphodynamic spin-up, starting from the 1995 measured bathymetry. The forecast analysis is based on only two 80 year scenarios, i.e. with 0m SLR, and with 2.63m SLR. Mind that the 2.63m refers to a global SLR that implies a SLR of 3.02m/century at the Western Scheldt mouth. We considered a linear SLR, where non-linear SLR runs showed only minor differences (see Röbke et al., 2020). “Current” DAD describes the DAD strategy applied in 2013-2014 (dredged sediment deposited in both, channels and shoal areas), while “Future” DAD describes a possible strategy where material is disposed mostly in the deepest parts of the channels and more in eastern regions upstream of Terneuzen, see Figure 2-1. In the forecast, the minimum depth in the DAD algorithm is defined with respect to a rising mean sea level, thus allowing accretion of the main channel. The nourishment scenarios describe a yearly nourishment of 750.000 m^3 on the beaches between Zeebrugge Harbour and Breskens (A), and of 250.000 m^3 along the Oostgat channel (B). No sand mining was imposed in the forecasts. To assess the potential impact of morphodynamic development, one of the forecast runs was morphostatic , i.e. without morphodynamic adaptations. To assess the potential impact of morphodynamic development, the forecast runs include a morphostatic run as well. A final scenario describes a possible large-scale landscape intervention by removing the Land van Saeftinghe (LvS) from the model.

Table 1 Overview of analysed runs

	Waves	SLR m/century	DAD	morphostatic	sandmining	nourishments
hindcast	in/ex	0	Current		x	in
forecast	in/ex	0/2.63	Current/Future			in/ex
forecast				x		
forecast (no LvS)	in	0/2.63	Current			in

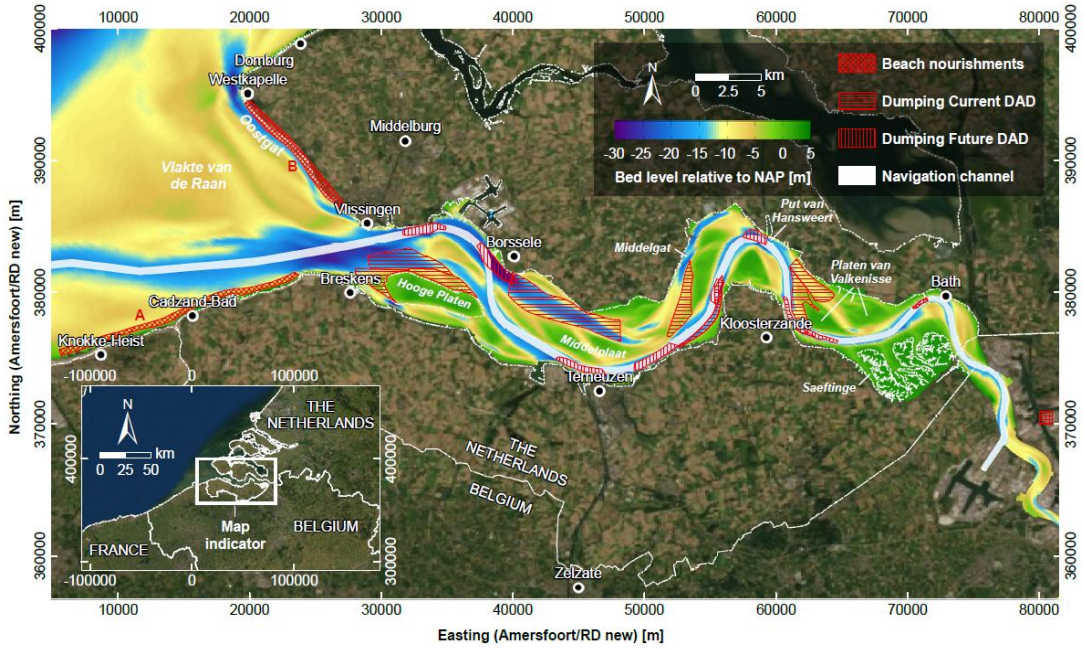

Figure 2-1. Disposal locations for the Current and Future DAD strategies as well as beach nourishment locations (A = beaches between Zeebrugge Harbour and Breskens; B = beaches along Oostgat channel) in the Western Scheldt estuary.

2.2 Hindcast data

The used bathymetric data consists of the Vaklodingen dataset of Rijkswaterstaat. This dataset combines single-beam and LiDAR measurements to define a 20x20 m raster (De Vet et al., 2017; Elias et al., 2023) that was then interpolated on the model grid for easy comparison with model results. The Vaklodingen dataset was available from 1955 to 2022, and it was decided to compare the model results and observations for the period 1965 to 2010 in 5-year intervals. Figure 2-2 and Figure 2-3 describe the areas considered. Because of its exceptional nature with relatively high grounds, the intertidal area in Land of Saeftinghe (LvS) was excluded from the hindcast analysis described in Section 3.1 (but is was included in the model runs). To prevent historic and modelled shoal migration crossing boundary polygons for sub-area analysis (like western, middle and eastern areas), the deeper parts of the main channel were used as boundary for the polygons defining sub-areas.

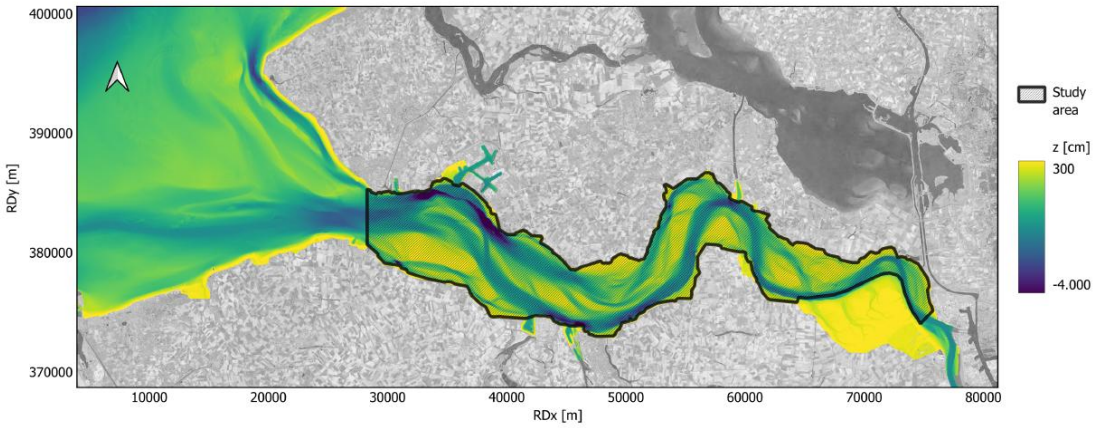

Figure 2-2. Polygon definition of the total study area of the Western Scheldt. Zones close to the shoreline were excluded because of incompleteness and/or likely errors. Source: Paternotte (2024)

Studying the behaviour of individual intertidal flats is difficult because of their migratory nature. Over the past sixty years, some intertidal flats have even merged or subdivided. For this reason, it was decided to analyse the evolution of these morphological features on a more regional level in three sub-regions. Using QGIS, polygons were defined for the western, middle, and eastern parts of the estuary (see Figure 2-3). Migration of modelled and measured shoals did not take place across these polygons.

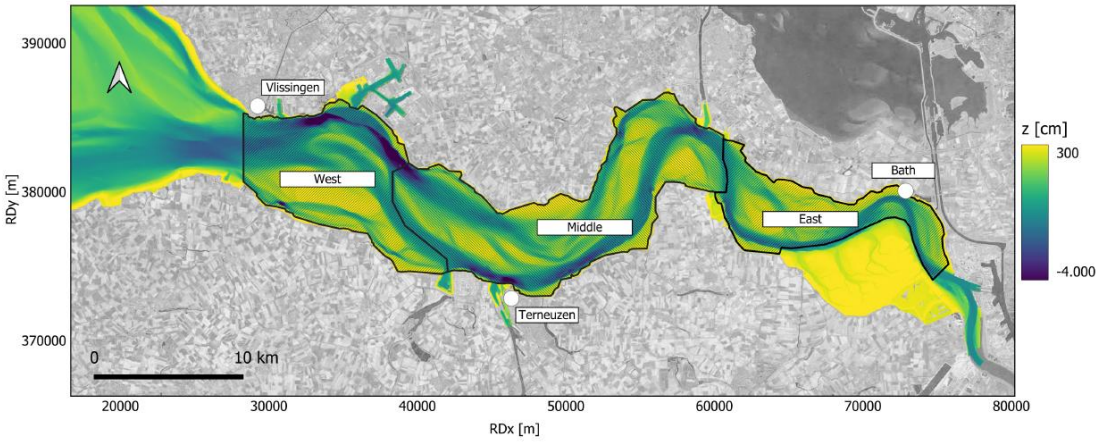

Figure 2-3. Polygons to study the regional evolution of intertidal areas in the Western Scheldt. The total region is the same as the polygon defined to study the total study area of the Western Scheldt. Source: Paternotte (2024)

2.3 Intertidal range definition

One can define intertidal range based on the water levels (HW, LW) required to define the intertidal area, where the intertidal range closely relates to the tidal range. However, the tidal range is not constant over time and along the Western Scheldt. Variations in the tidal range have both periodic causes, such as the spring-neap tidal cycle and the nodal tidal cycle (18.6 years), and random causes such as storms. In addition, the tidal range increases from west to east so that a wider range of intertidal bed levels needs to be considered towards the east.

Two measurement-based definitions of the intertidal range have been considered, i.e. based on the mean high water and mean low water and based on the 50% and 30% highest high water and lowest low water levels. A comparison of the definitions showed that the 50% and 30% margins where higher (lower) than the high (low) water level during neap tides. Also, extreme events such as storms will have a larger influence on the value of the 30% highest high waters and lowest low waters. For this reason, the intertidal range defined by the averages of the 50% highest high waters and lowest low waters were selected for the validation of the model in this report.

Linear interpolation along the main channel of the average 50% high and low water levels is performed between Vlissingen, near the mouth, and Bath, at the east of the estuary. A linearly increasing tidal range for this part of the estuary was also found by the modelling study in Robke et al (2021) and measurements (e.g., Schepers et al., 2018). To derive the 50% HW and 50% LW for the forecasting phase of this study water levels were extracted from the model instead of measurements. For this purpose, morphostatic simulations were carried out for one-year periods for different mean sea levels. The 50% maximum high-water level and minimum low-water level were computed for 13 different stations placed along the estuary, from Vlakte van de Raan to Schelle. In between stations, linear interpolation was carried out.

3 Results

3.1 Hindcast

3.1.1 Comparison for the whole region of the Western Scheldt

Comparing observed and modelled trends of intertidal area, Figure 3-1 shows clear differences in height, location, and morphodynamic evolution. In particular, the model results show intertidal area evolving around km 53 and km 63 that is not observed in the measurements. This is probably due to DAD algorithms, especially the disposal implementation. Model results including waves generally lead to smoother and larger patches of intertidal area. Furthermore, including waves leads to relatively high deposition rates around km 56 at the southern banks, probably related to erosion of disposal induced flat area around km 53.

The Vaklodingen dataset initially shows a general increase in the elevation of the intertidal flats (*Figure 3-2*, *Figure 3-3* and Figure 3-4) while the elevation remains more stable after 1990. The lowest elevations (below -1 m NAP) show more variability on the elevations of the intertidal flats over time. From 1965 to 1970 there is a major gain in intertidal area. Between 1980 and 1990 there is a considerable decrease in intertidal area. It then remains almost constant till 2000 and decreases again till 2010. Overall, the total intertidal area in 2010 is less than in 1965. In addition, with time, the slope of the hypsometry curve becomes steeper in the lower regions.

The no-waves and waves hindcasts show a much slower increase in elevation of the intertidal flats over time, albeit that the 2010 profiles have similar elevations as the measured profiles. Also, the hindcasts lead to less elevation at lower levels (<-1m) and other, smaller variations in area. Remarkably, the wave hindcast promotes more accretion at higher levels (>1m). Similar to the measurements, the hindcasts show a steepening of the hypsometric curve at lower levels. For 2010, the hindcasted hypsometry probably resembles the measured hypsometry best.

Figure 3-3 and *Figure 3-4* show that the model hindcasts the finally observed 2% decrease in intertidal area and the 30% increase in mean intertidal area height over the 1965-2010 period quite well. However, over the 45 year period the maximum model error is of similar magnitude as the observed variations (~10% of the present area). The model first underestimates the increase in intertidal area and then overestimates the decrease. The modelled increase in mean height is underestimated first decades but then the error becomes negligible after 45 years. Adding waves generally leads to a difference in error of maximum 5% of present area and height, sometimes improving the model performance and sometimes not.

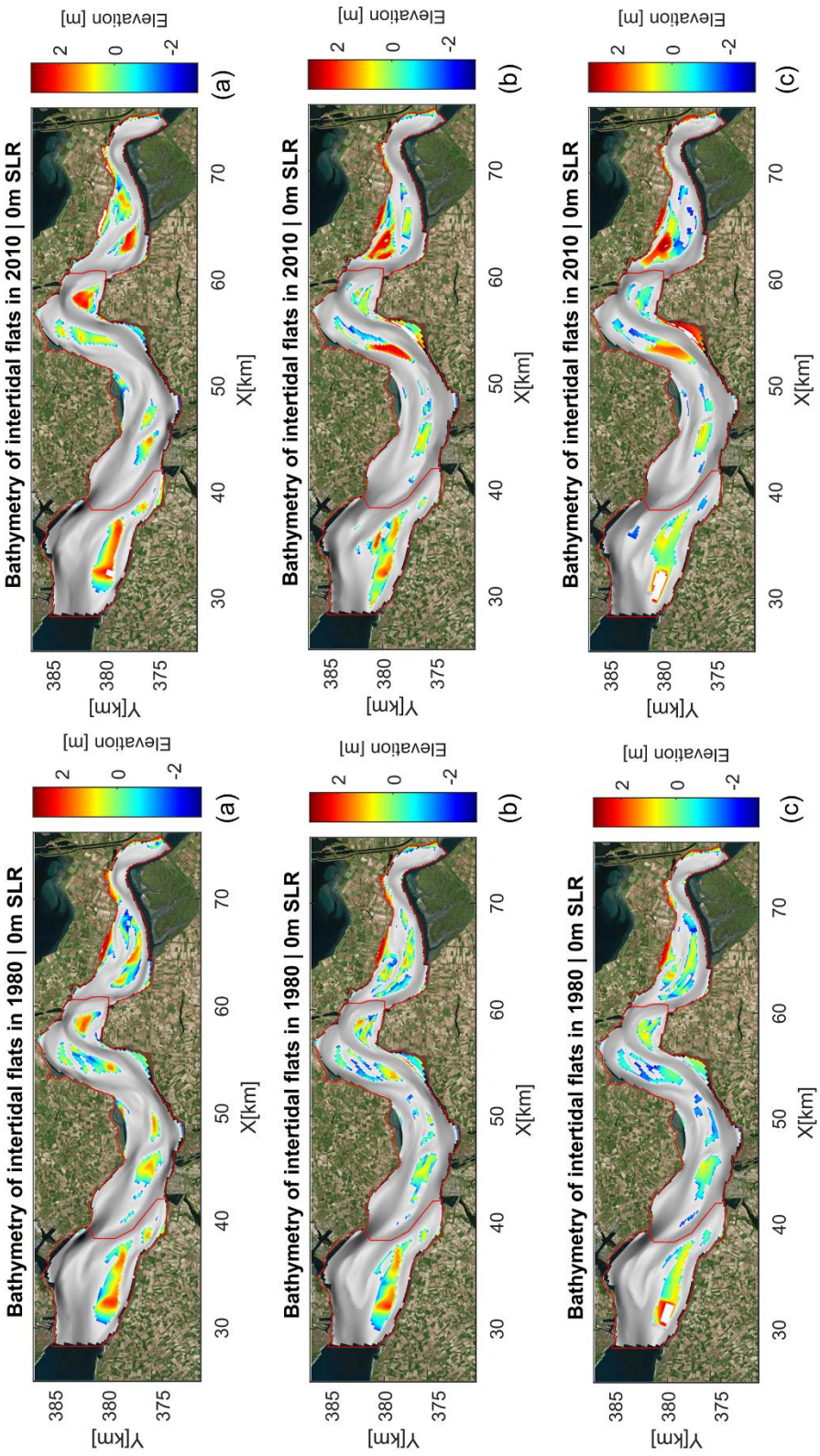

Figure 3-1. Evolution of intertidal areas based on the Vaklodingen (a), the hindcast without waves (b) and the hindcast with waves (c). Thee polygons used to study the different regions within the estuary are shown in red. The white area near the mouth for the hindcast with waves stems from morphodynamic development higher than high water, probably due to the morphological factor.

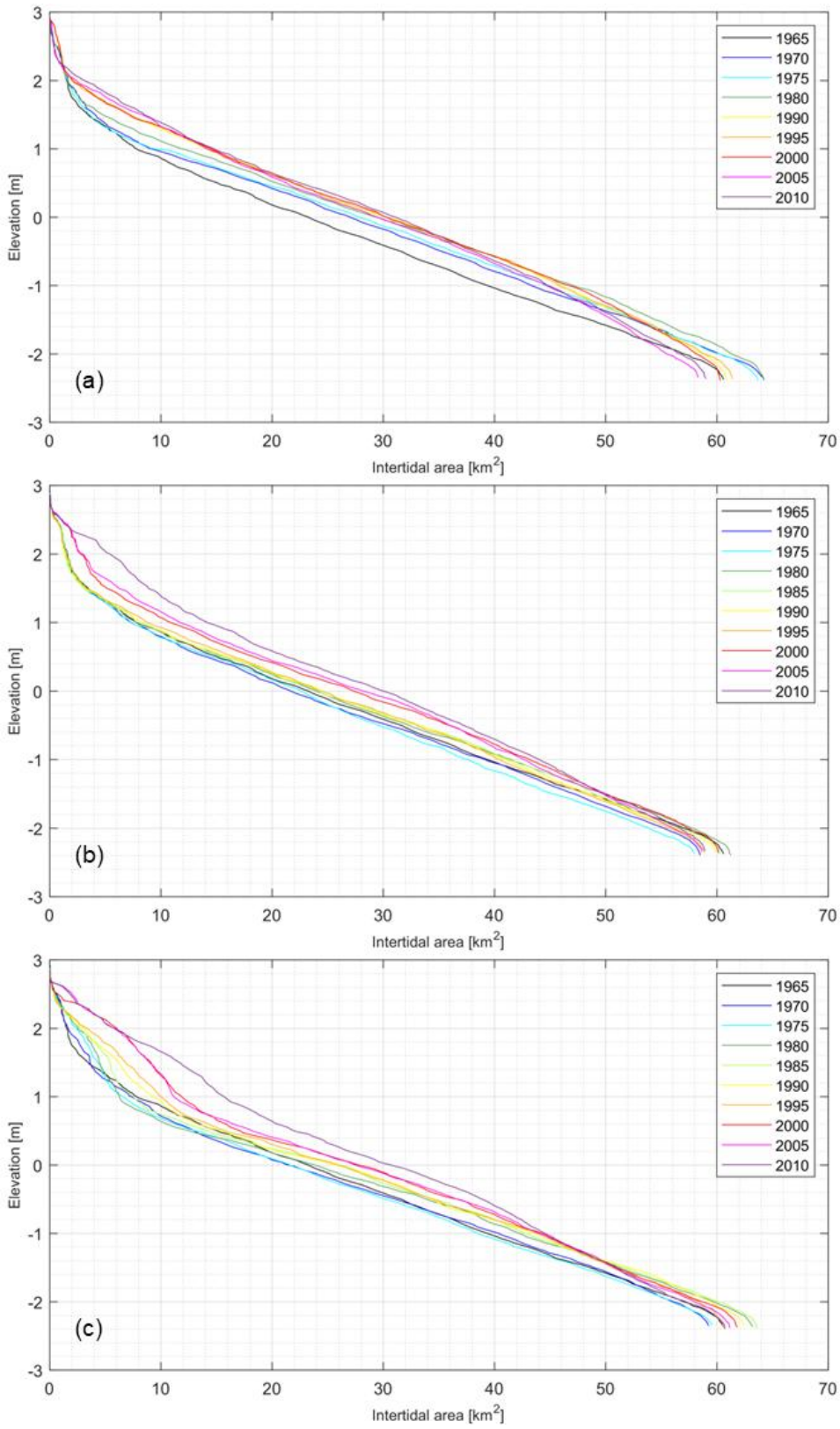

Figure 3-2. 1965-2010 Hypsometric curves covering entire domain excluding LvS of the (a) Vaklodingen dataset; (b) no-wave model results (c) wave model results.

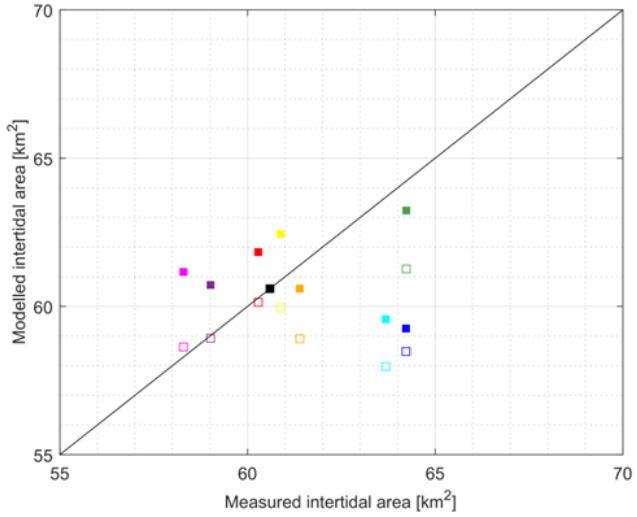

(a) Measured compared to modelled intertidal area

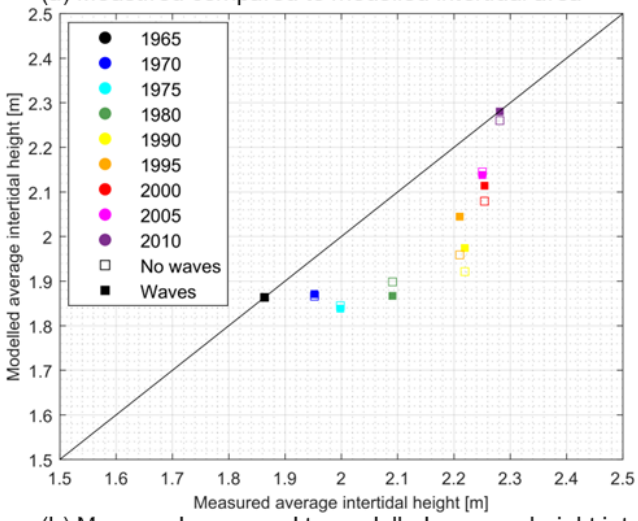

(b) Measured compared to modelled average height intertidal area

Figure 3-3. (a) Intertidal area and (b) average intertidal height based on the Vaklodingen and the two model hindcasts (excluding LvS). The line at 45° with respect to the horizontal axis shows if there is a perfect match between measurements and model results. Figures consider entire domain excluding LvS.

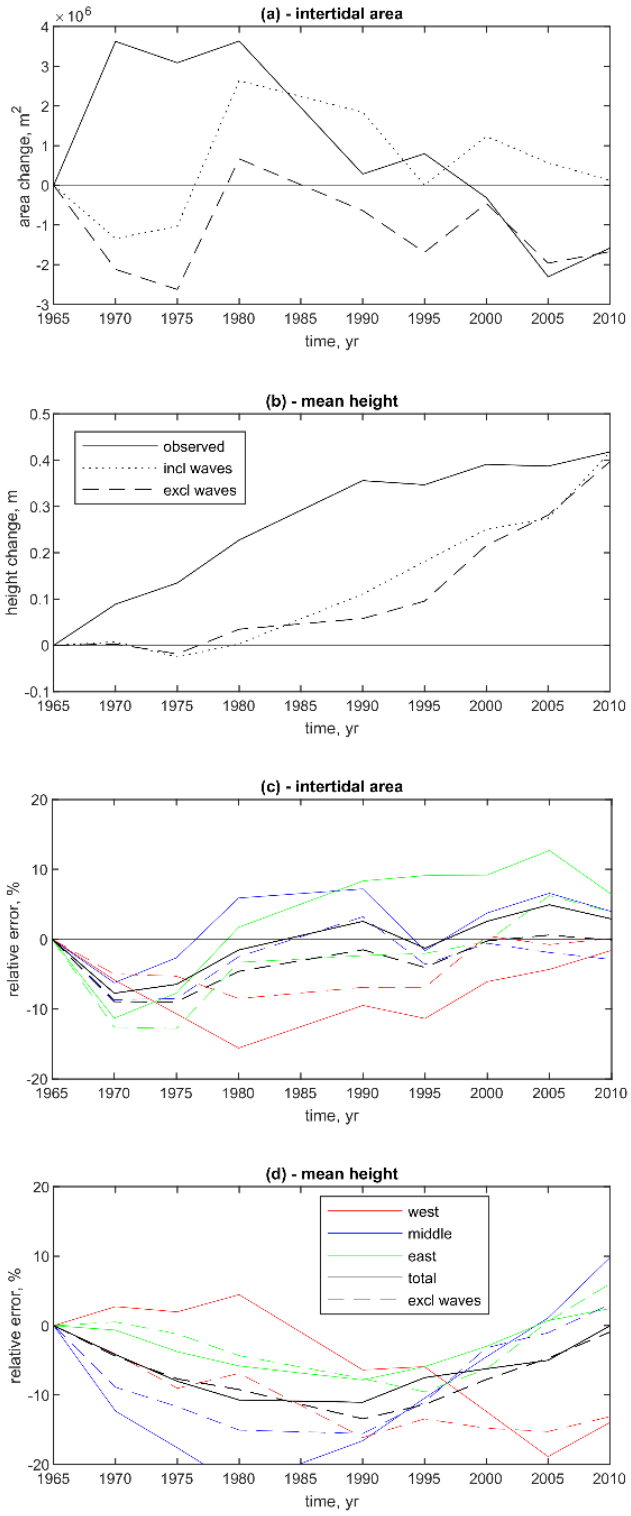

Figure 3-4 (a) Cumulative intertidal area change; (b) Cumulative change in mean intertidal area height; (c) area relative error (model_area-observed_area)/observed_area; (d) mean height relative error (model_mean height-observed_mean height)/observed_mean height, (excluding LvS). Figures consider entire domain excluding LvS.

3.1.2 Comparison for sub-regions of the estuary

On a sub-regional level, there are larger errors (Figure 3-4 c,d) compared to the total area analysis. To some extent, the errors over sub-regions average out. Also, there is more variability over time in the hypsometry, intertidal area and mean height (Figure 3-5 and Figure 3-6) than in the total region of analysis.

The model results maintain aspects of the Vaklodingen observations such as the slightly concave hypsometry in the west, accretion of the upper intertidal parts in the middle and accretion of the main profile in the east. Still, modelled trends in hypsometric evolution may occur at different rates and magnitudes. The one-directional wave climate has a major impact on the hypsometry in the western part, flattening the hypsometry around MSL (Figure 3-5a). This is not apparent from the Vaklodingen. The wave impact in the eastern, wave-sheltered area is more limited (Figure 3-5c). Excluding waves generally shows more resemblance with observations.

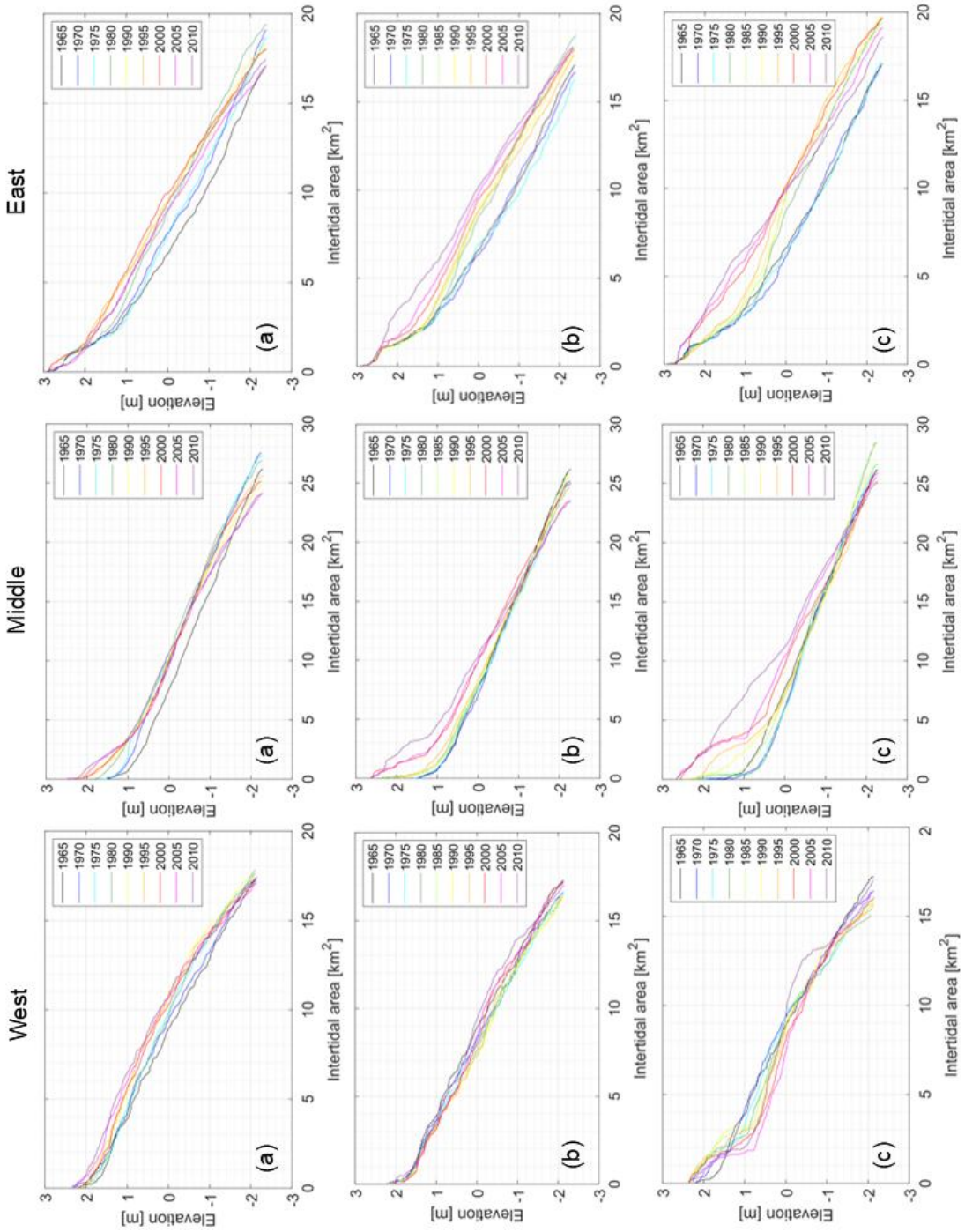

Figure 3-5 Hypsometric curves (excluding LvS) for the western, middle and eastern parts of the Western Scheldt for the Vaklodingen dataset (a), and the hindcast model results without (b) and with waves (c).

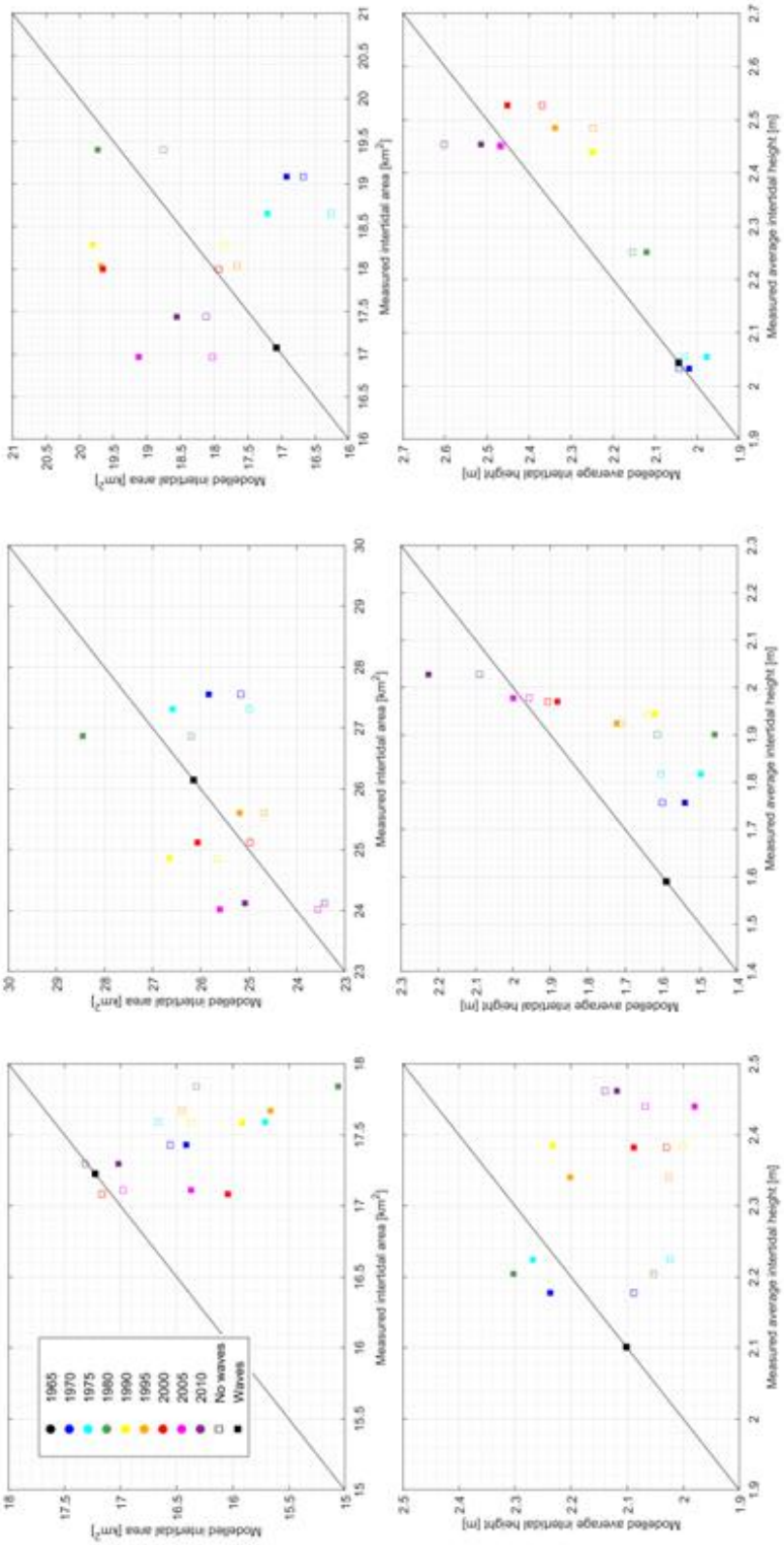

Figure 3-6 Intertidal area (upper row) and average intertidal height (lower row) for Vaklodingen (x-axis) and model hindcasts (y-axis) for west region (left column), middle region (middle column) and east region (east column), excluding LvS. The line at 45° with respect to the horizontal indicates a perfect match between measurements and model results.

3.2 Forecast

Figure 3-7 and Figure 3-9 show that, after 80 years and without SLR, the amount of intertidal area increases. The regions with higher elevations coincide with the places where sediment is disposed according to the Current DAD. It can be observed how Schaar van Valkenisse fills up due to disposal. The Everingen channel also intensively fills up to the point that new intertidal area is created. Including waves leads to less high elevations in the intertidal areas due to direct disposal. This means that waves help in eroding and spreading the sediment. Only the DAD strategy causes major differences. It is evident that there is less intertidal area in the case of Future DAD. This is expected as Future DAD does not directly dispose on shoals.

Figure 3-8 shows that Land van Saeftinghe (LvS) largely remains intertidal under extreme SLR since it consist of relatively highly elevated intertidal area compared to the rest of the estuary. This region consist already of relatively highly elevated intertidal area compared to the rest of the estuary, which explains it resistance to drowning under SLR. The intertidal areas closer to the mouth and the central part of the estuary decrease considerably. Current DAD helps to counteract drowning of the intertidal areas by placing sediment in the subtidal regions nearby. Including waves in the model leads to more intertidal area in larger patches. Adding nourishments shows negligible differences.

Furthermore, Figure 3-9 and Figure 3-10 show that;

- At the beginning of the simulation (but after the morphodynamic spin-up) and throughout the simulation period Current DAD or including waves lead to more intertidal area (~10% after 80 years).
- Under extreme SLR, the intertidal area decreases over the years. In the worst-case scenario (Future DAD, no waves, no nourishments), roughly 40% of the intertidal area is lost. Intertidal area decline is largest under Future DAD. Under moderate SLR scenarios (1.1 and 1.96 m SL for 2100), there is less loss of intertidal area (Figure 3-11 and Figure 3-12).
- Regardless of the applied DAD strategy, nourishments at the beaches of the mouth of the Western Scheldt have an insignificant contribution to the intertidal area (also when there is No SLR). Only with SLR and under Future DAD, a small nourishment effect is noticed, especially from 2080 to 2100.

The grey lines in Figure 3-9 and Figure 3-10 show the impact of excluding morphodynamic development in the runs leading to generally less intertidal area with a difference after 80 years ranging from 10% (no SLR) to 20% (SLR). The morphostatic results resemble the Future DAD, no waves, case most. This is logic since Future DAD only disposes only in deeper channels feeding the intertidal flats less than current DAD

To explore the possible impact of a large scale landscape intervention, we performed an additional run where we excluded Land van Saeftinghe from the model (red lines in Figure 3-9 and Figure 3-10). Overall, the trends for No SLR and extreme SLR are similar except for the contribution of Land van Saeftinghe (LvS) to the total amount of intertidal area. There is more (relative) gain of intertidal area when LvS is not in the model in case of no SLR. The reasons are not fully understood but may be attributed changed tidal characteristics leading to disposed sediment depositing more at intertidal flats. Also LvS may be a sediment sink. Excluding LvS will then favour sediments to deposit at other intertidal flats. Under extreme SLR, the loss of intertidal area is larger when LvS is not in the model. This may be attributed to LvS being relatively highly elevated and less subject to drown even under extreme SLR. Another explanation may be that excluding LvS leads to less tidal prim, lower velocities, smaller sediment transports and thus less capacity to build intertidal flats. Finally, Figure 3-11 and Figure 3-12 show that gradually increasing SLR leads to a gradual and proportional decrease in intertidal area.

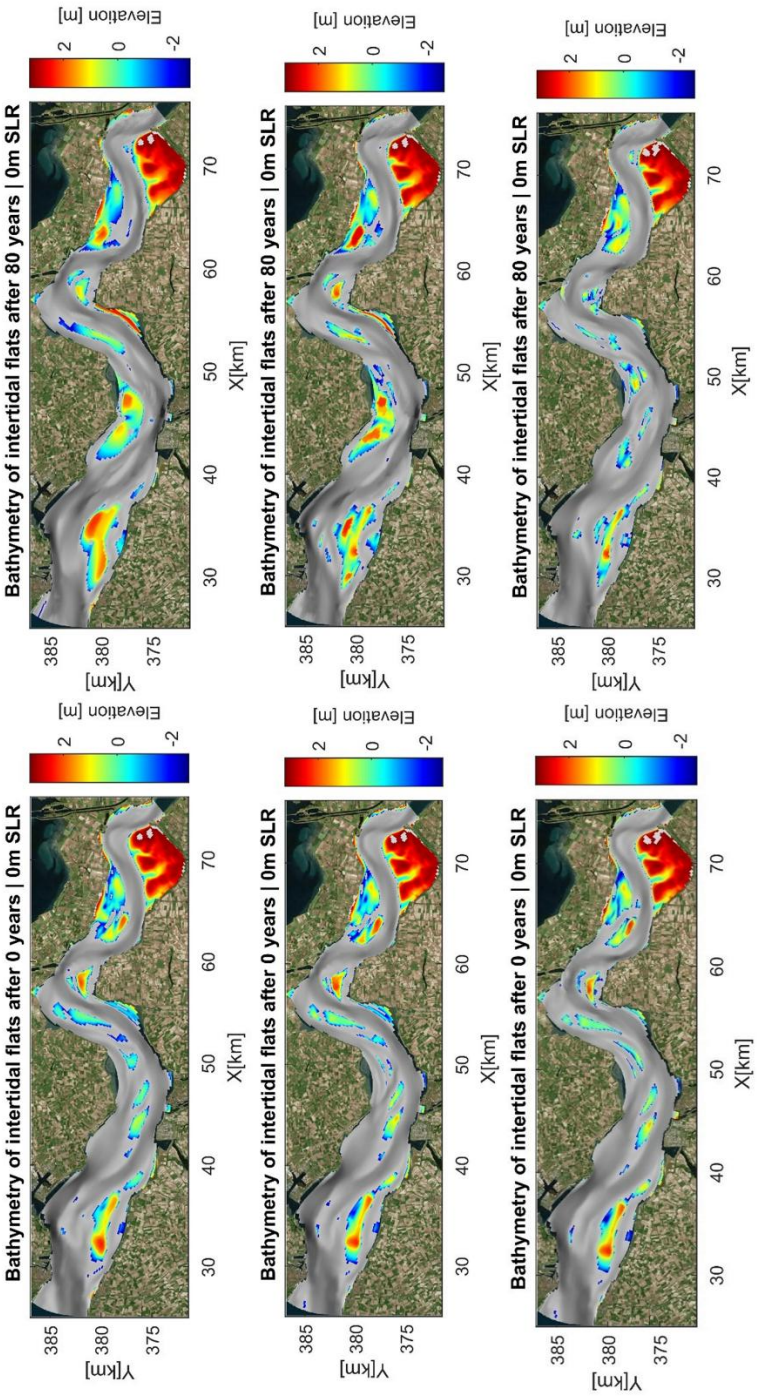

Figure 3-7 Maps showing the evolution of intertidal areas in the Western Scheldt under No SLR. First column shows the initial bathymetry after 25 year spin-up; the second column presents results after 80 years. The top panel shows the results for the case with Current DAD, with waves and without nourishments; the middle panel includes Current DAD, without waves and without nourishments; and the bottom panel shows the case with Future DAD, without waves and without nourishments.

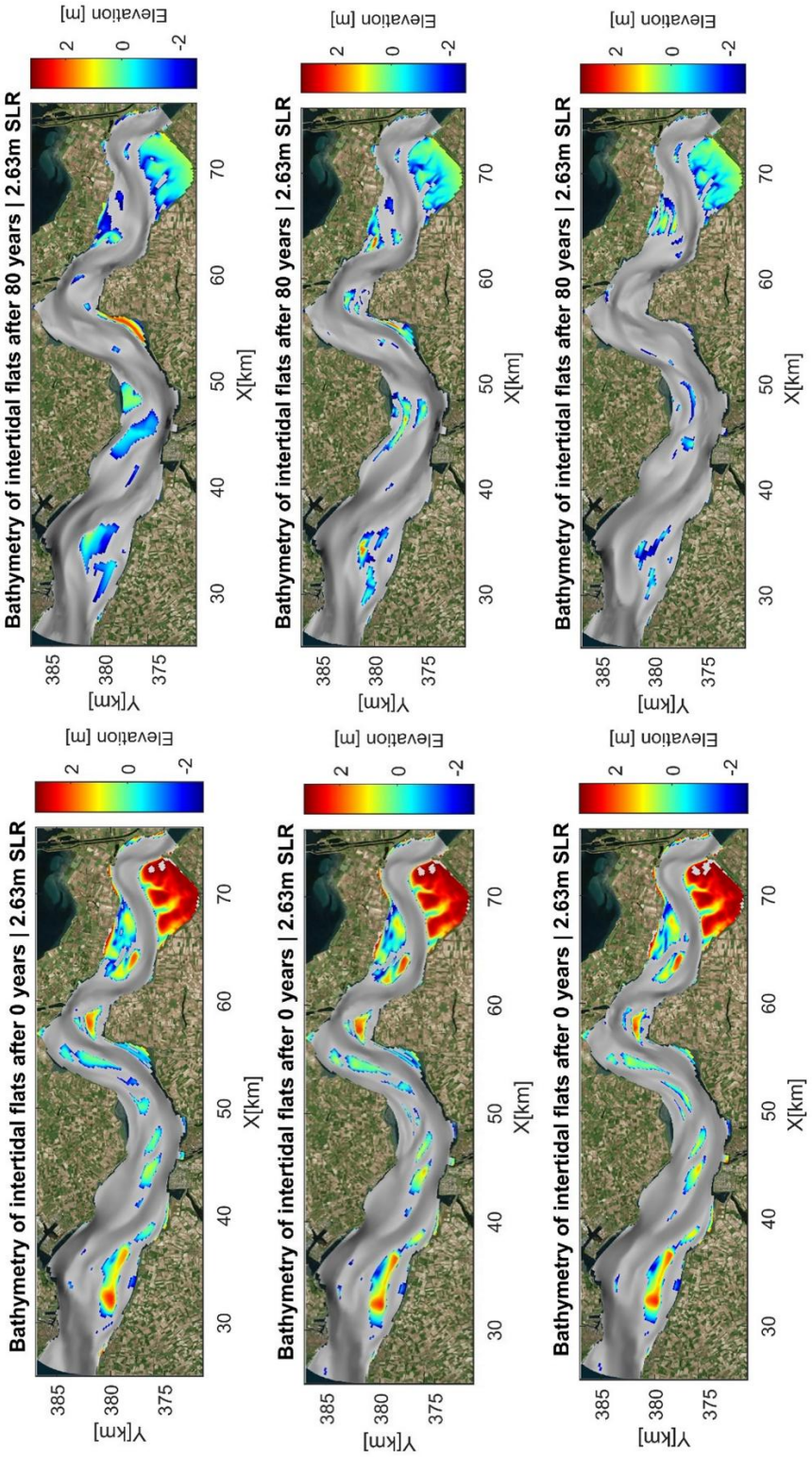

Figure 3-8 Maps showing the evolution of intertidal areas in the Western Scheldt under extreme SLR. First column shows the initial bathymetry after 25 year spin-up; the second column presents results after 80 years.. The top panel shows the results for the case with Current DAD, with waves and without nourishments; the middle panel includes Current DAD, without waves and without nourishments; and the bottom panel shows the case with Future DAD, without waves and without nourishments.

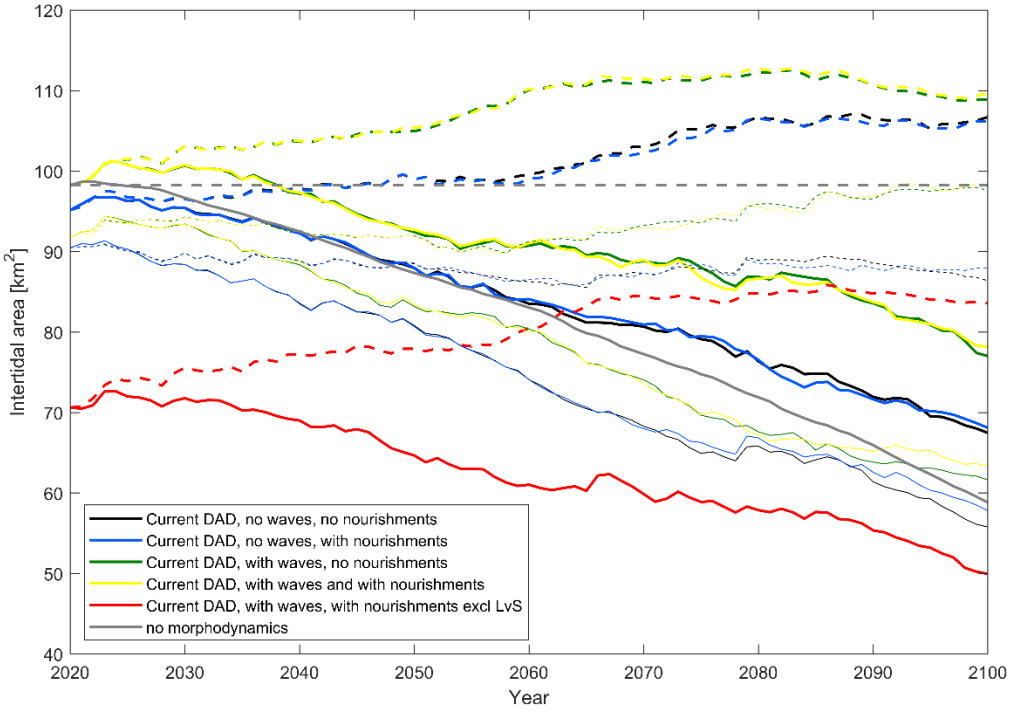

Figure 3-9. Evolution of intertidal area in the Western Scheldt from 2020 to 2100 under No SLR (dashed lines) and extreme SLR (solid lines). Mind that the small set-of at t=2020 is due to the 25 year morphodynamic spin-up applied. Thick (Thin) lines refer to Current (Future) DAD.

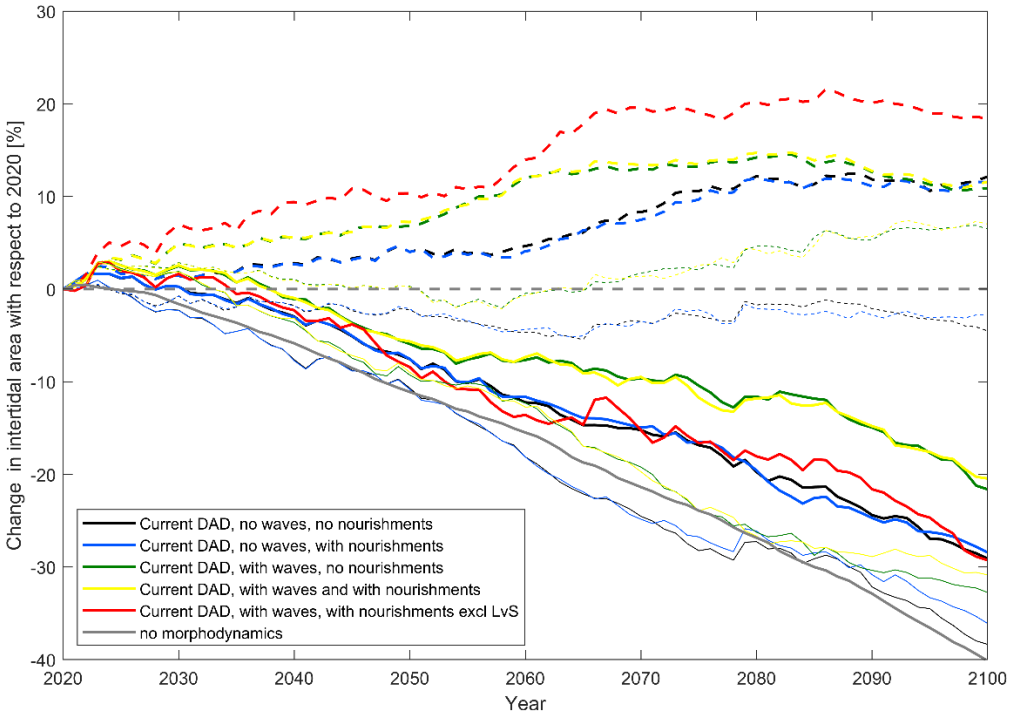

Figure 3-10. Change of the intertidal area in % with respect to 2020. The dashed lines represent No SLR cases, and the solid lines extreme SLR cases. Thick (Thin) lines refer to Current (Future) DAD.

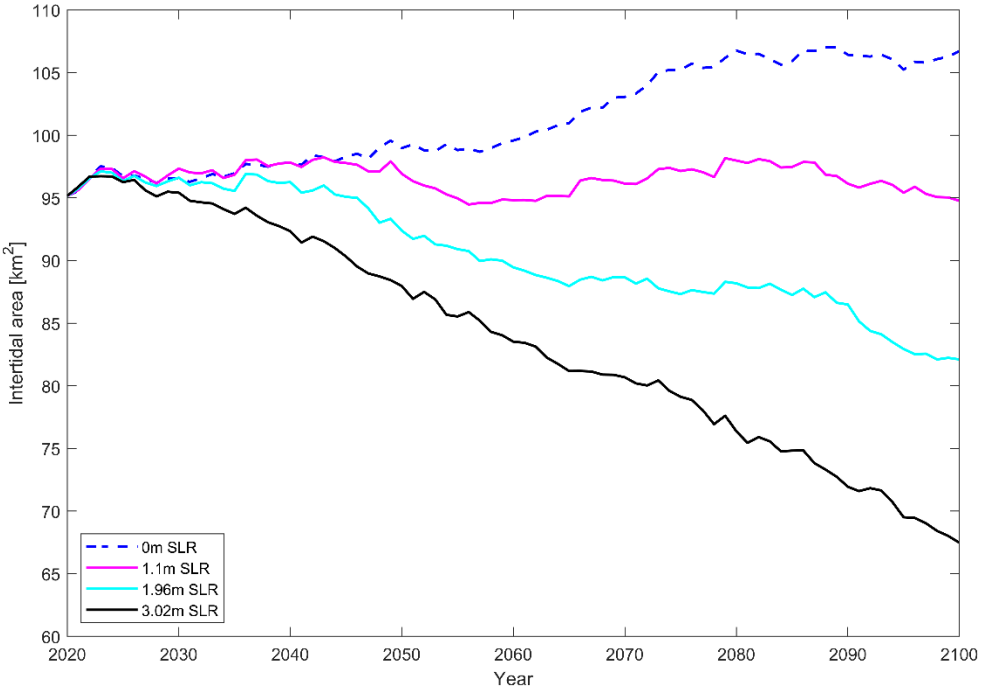

Figure 3-11. Evolution of intertidal area in the Western Scheldt from 2020 to 2100 under different SLR scenarios (0 m, 1.1 m, 1.96m and 3.02 m). Current DAD, no waves and no nourishments is applied in all the simulations.

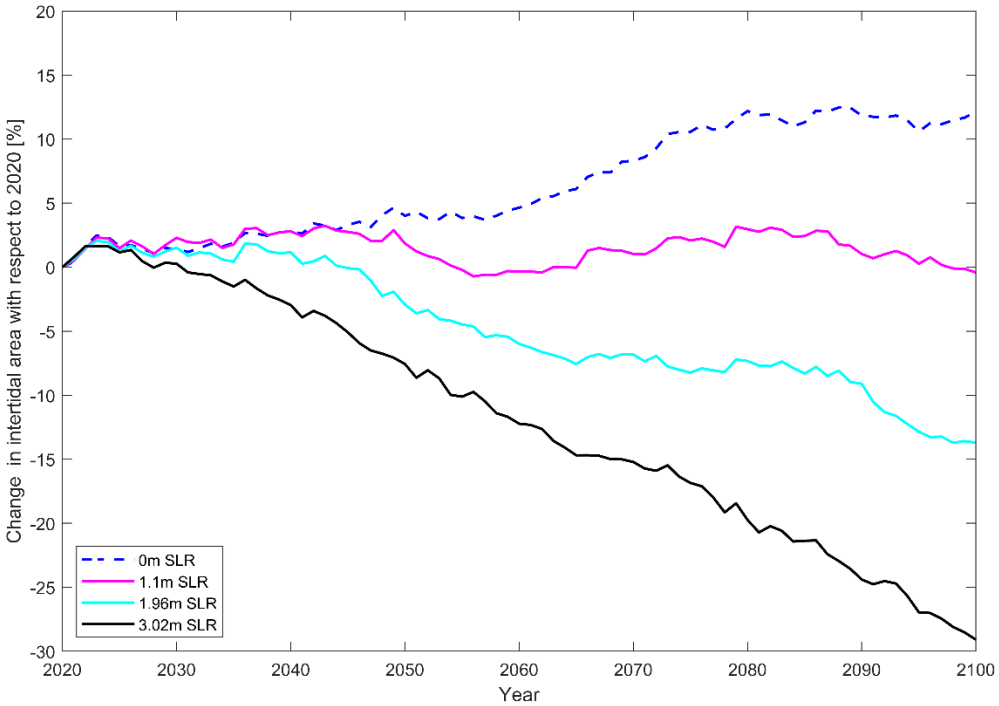

Figure 3-12. Change of the intertidal area in % with respect to 2020 for different SLR scenarios (0 m, 1.1 m, 1.96m and 3.02 m). Current DAD, no waves and no nourishments is applied in all the simulations.

4 Discussion

4.1 Hindcast

4.1.1 Effect of dredging and disposal set-up in the model

One major factor influencing the hindcast results is the definition of dredging and disposal in the model. It is known that there were three major deepening phases of the main channel of the Western Scheldt in the period of analysis. The first and major one, between 1973 and 1976, the second one between 1997 and 1998, and the last one in 2010. Besides the dredging depths, for each deepening phase, the locations where sediment was disposed to also differed. For the first phase, the dredged material was disposed in the secondary channels nearby and along the eroding channel banks of the navigation channel. For the subsequent phase, disposal took more often place in the secondary channels of the western part of the estuary, hence there was a human-induced net western transport of sand. For the last deepening period, disposal was carried out in some parts of the secondary channels, the deepest parts of the main channel, and in the shallow subtidal regions, seaward-located tips of the three intertidal shoal complexes with various disposal techniques (Elias et al., 2023). Although the deepening phases were included for the dredging (maintaining different dredge depths over three different periods), the disposal areas and distributions were kept constant for the hindcast based on the 2013-2014 strategy.

Dredging and disposal also had another major limitation in the model. For each of the deepening phases, a specific day within the simulation was defined as the moment in which each of them had to be executed. Then, all the dredging and disposal occurred in one computational timestep for an entire region instead of locally scattered activities over a prolonged period of time (e.g., months-years as it is in reality). This led to abrupt and unrealistic changes in the bed levels that would take quite some time to smooth out. Figure B. 3 shows two examples in which sediment was disposed in the main channel leading to a recognisable hump.

In addition, disposal contributed to large (modelled) sedimentation north of Hooge Platen, in the Everingen channel, Plaat van Walsoorden and Rug van Baarland. The large relative increase in intertidal area in between 1975 and 1980 in the east of the Western Scheldt ((km 63 in Figure 3-1) is to direct disposal in the Schaar van Waarde which caused infilling of this channel in the model. After infilling of this channel, further disposal of sediment caused the rise in intertidal area, which explains the increase in height for elevations above 0 m NAP from 1980 till 2010. Disposal near Rug van Baarland also caused the accelerated rise in intertidal height between 1980 and 2010 (km 53 in Figure 3-1).

The sand mining rate was assumed to be constant during the hindcast based on the average yearly sand mining volumes in the period 1963-2012 (i.e. 2410100 m^3/yr). The sand mining definition with averaged values over the 45 hindcast period, is also a simplification with respect to how it was actually executed in the past with potential consequences for the model performance although we estimate the sand mining impact to be less than the DAD impact.

4.1.2 The effect of assumptions for tidal range

For this study, the average 50% highest high water and lowest low water from measured water levels were used to compute the intertidal range (i.e. the tidal frame), where the intertidal area was defined as the area present in that range/frame. A sensitivity analysis on the impact of another definition was not carried out. Nevertheless, it can be argued that the effect would be limited since the hypsometry curves show a very steep slope for the lowest low waters and highest high waters (see Figure 3-2 and Figure 3.4). Besides, the intertidal range definition was equal for measured and modelled bed levels, not impacting the analysis on model performance.

By using a constant value of 50% highest high water and 50% lowest low water for the entire period of analysis, the variability in the water levels due to the tidal nodal cycle of 18.6 years is excluded. The tidal nodal cycle causes differences as large as 20 cm in the tidal range at Vlissingen, and 40 cm at Bath (Figure B. 4). However, it was found out that if the yearly variability in the water levels were taken into account, the impact on the trends of the intertidal area considered remained minor (see Appendix B.4).

Due to computational restrictions, the tidal nodal cycle was not implemented in the numerical model. Instead, a timeseries of one year (2012 in this study) based on the astronomical components (32 in total) was used as water level seaward boundary conditions. Excluding the tidal nodal cycle can influence the modelled bed levels since it is expected that a larger tidal range leads to more sediment transport and (delayed) morphodynamic response. For the studied period, the maximum difference between the minimum and maximum tidal range by nodal cycle variations was 40 cm, which seems not negligible. Nevertheless, considering the long-term (> decades, multiple nodal cycles) analysis of the current study, the effect of the nodal cycle on the bed levels may remain limited. Also, the error made would relate to absolute values whereas the emphasis of this study lies in the evolution over time. The largest absolute error would be expected if the year that was taken to derive the water levels (2012) was at the top or bottom of the cycle. Figure B. 4 shows that the tidal range in 2012 is above average, but not at the extreme. Furthermore, we assume that delayed morphodynamic developments as the results of the tidal nodal variations remain limited, (see also Jeuken et al., 2003).

4.1.3 Inclusion of wave modelling

From a qualitative perspective, based on model results, including waves leads to less patchiness of intertidal area, slightly more deposition on higher grounds, max~4% more area and generally slightly higher (1~3%) levels. Resemblance with observations varies over time and location where including waves sometimes performs better and sometimes performs worse, while trends in performance of runs including waves roughly follow performance trends of runs excluding waves. For example, *Figure 3-6* shows that waves lead to higher and narrower flats in the western part near the mouth (generally more wave action) and wider, often lower flats in the eastern, wave-sheltered part. This suggests that waves do not fundamentally impact model performance and intertidal flat development, although applying a more advanced wind and wave climatology (directions, magnitudes) could improve model results.

Model results seem to challenge the idea that tides build flats whereas waves erode flats eventually leading to an equilibrium hypsometry. Rather, model results suggest that tides are the main forcing mechanism building up shoals and intertidal flats, whereas waves play a secondary role by redistributing sediments over the intertidal flats and making them wider. Earlier research suggested that intertidal flats would also be lower under waves action (Zheng et al., 2021, Elmilady et al., 2022). The fact that our model leads to generally (but also limited) higher intertidal flat levels may be attributed to spin-up effects where an initial bathymetry is adapting and redistributing sediments to prevailing schematized model forcings. The (limited) wave impact may differ depending on the shoal location (close to the mouth or inland) and

characteristics (fringed or not fringed along shorelines), especially when SLR scenarios are considered. Closer sensitivity analysis should reveal if numerical issues like the morphological factor value also play a role in the modelled intertidal flat heightening.

4.1.4 Interpolation of Vaklodingen dataset in the model grid

The Vaklodingen dataset was interpolated to the grid of the Delft3D-Scheldt-SLR model. Since the model grid has a resolution that is a factor ten lower than the one from the Vaklodingen, there is some data loss. It was found that carrying out the interpolation led to a decrease of 3% in the total intertidal area computed using the polygon enclosing the whole study area of the Western Scheldt (see Figure 2-2). The trend in the hypsometric curve is preserved after the interpolation. Therefore, the coarser grid resolution does not play a large role in the differences between the model outcomes and the measurements. See B.2 for the detailed comparisons. The impact of increasing model grid resolution is yet to be investigated.

4.1.5 Impact of assumptions made for the model set-up

SLR was not considered in the model hindcasts (period 1964-2012). However, the water level data from the measurement stations in Vlissingen and Bath suggest a SLR of approximately 1 cm every 6 years. Literature suggests that when SLR rates are low (below a critical value), basins adapt their bed levels to follow it in order to keep dynamic equilibrium (Wang et al., 2018). SLR can thus heighten, but also narrow intertidal flats depending on the morphodynamic adaptation rates. We assume that SLR impact during the hindcast has been limited compared to autonomous developments and DAD interventions.

Only one sediment fraction was accounted for in the model, sand with D_{50} of 200 µm. While sand is the dominant fraction in the channels of the Western Scheldt, there is quite some presence of mud in the intertidal areas. Then, excluding mud is probably not appropriate when using the model to study the influence of SLR on intertidal areas. First, because sand-mud interactions are not modelled. For example, mud forms a layer that protects sand from easily being eroded (Röbke et al., 2020). And second, mud is a crucial component in intertidal area. Since it is composed by very fine particles, it travels longer distances, which allows remote zones in the basin to keep up with SLR (see also Wang & Van Der Spek, 2015; Elmilady et al., 2020, 2022). Especially, mud would settle at the most landward and higher areas eventually enabling marsh development and a change in sediment entrapment processes. These processes are not considered either.

Additionally, the model configuration was 2D, and salinity and temperature differences were not considered. These factors contribute to differences with respect to reality. However, the effect that they have on the morphology, the elevation and location of intertidal areas is unknown.

4.2 Forecasts

Figure 3-9 shows that Current DAD maintains more intertidal area than Future DAD. In the Current DAD, disposal takes place in both channels and shoals of the estuary, while for the Future DAD, disposal happens mostly in the deepest parts of the channels. Then, the model disposes sediments in areas with shallow shoals leading to more intertidal area at the end of the spin-up (2020, start of the reported results) and throughout the entire simulation. Not having a direct disposal on the shoals in case of the Future DAD explains why intertidal area decline is larger than for the Current DAD. Still, Röbke et al. (2020) show that Future DAD leads to more sediment maintained in macro cells 3-5 suggesting that disposed sediments mainly deposit in channels deeper than the prescribed dredging depth or on shoals under low water.

The model results also suggest that beach nourishments (outside the estuary) have a limited effect on the response of intertidal areas in the estuary under SLR.

Waves generally lead to more intertidal area (whereas intertidal area height was not evaluated). Under Current DAD including waves maintains more intertidal area under SLR and noSLR, although there is no difference after 80 years anymore in case of noSLR. Including waves under Future DAD shows similar behaviour, although the effect under SLR is less pronounced.

5 Conclusions and recommendations

This study aims to assess the performance of process-based morphodynamic modelling (Delft3D) in predicting the evolution of intertidal flats in the Western Scheldt and to explore possible impact of sea level rise (SLR) and dredge-disposal strategies on intertidal area evolution. A key underlying question is whether a process-based modelling approach is suitable for predicting the morphodynamic evolution of intertidal flats. The model's process formulations, initial conditions, and boundary forcing are limited and schematized, leading to deviations from observations. The question on model performance can be answered separately for the hindcast and forecast periods.

5.1 Hindcast

Model performance has been analysed in terms of the evolution of intertidal area patterns, hypsometry, area, and mean height. The modelled evolution of intertidal flat patterns shows quite some differences with observations. In particular the modelled disposal generates a clear signal of new intertidal area that is not observed in reality. Averaged over larger regions, the model has difficulty reproducing observed variations in intertidal area and height. Adding waves generally leads to differences of maximum 5% in terms of area and mean height, sometimes improving the model performance and sometimes not. The difference between model results and observations is generally worse (max 15% of the present values) when subregions are analysed, implying that regional differences in model performance partly average out in the total area analysis.

This analysis suggests that observed variations over time and spatial domains are not well reproduced, and that model results potentially include morphodynamic trends that may lead to systematic biases in longer term predictions. However, one could also argue that the model does not generate unrealistic morphodynamic development trends and that model results remain within a certain range of observed values. Improvements in model setup are possible, justifying additional research, including a more complex wave climatology, more advanced DAD operations, and adding mud and 3D dynamics.

5.2 Forecast

The 80-year model forecast shows a clear declining trend in intertidal area for various DAD and wave scenarios under 3m/century SLR (-20 to -40%), with the decline being proportional to SLR rates. No-SLR scenarios maintain more intertidal area over 80 years (-5 to +20%). The changes under extreme 3m/century SLR are larger than the model error prevailing during the hindcast. Lower SLR scenarios have an impact similar in magnitude to the hindcast error, making it more difficult to distinguish SLR impact from model uncertainties, at least for the 80 timeframe considered. Model results show that a strategy that disposes more sediments in the eastern part and deeper sections of the main channel leads to about 10% more intertidal area loss than under a strategy that disposes near intertidal area throughout the estuary.

5.3 Recommendations

To improve the performance of the model in predicting the evolution of intertidal areas in the Western Scheldt, the following implementations are recommended:

- **Update DAD algorithms**: Deepening phases of the access channel should be more accurately replicated in the model set-up. This includes revisiting and improving dredging and disposal area definitions, spreading dredging and disposal over longer

periods (as happens in reality), and imposing actually measured dredging and disposal volumes instead of model-generated volumes.

- **Enhance model setup**: Add SLR for the hindcast period, incorporate more sediment fractions (e.g., other sand fractions and mud), include 3D dynamics (i.e. salinity gradients and secondary flow), and implement a more advanced wind/wave climatology. Preliminary runs with a coarse 3D model show that 3D effects potentially have a large impact on the morphodynamic developments.
- **Validate hydrodynamics**: Hydrodynamic validation of the 3D 6th generation FM Western Scheldt model is ongoing. Morphodynamic tests with the 6th gen 3D model using Delft3D FM software show promising results. A hindcast performance analysis of this morphodynamic 3D model is recommended, similar to the bathymetric data-derived sediment budget and methodology described by Elias et al. (2023).

In general terms, concerning the impact of DAD and SLR on the evolution of intertidal areas in the Western Scheldt, the following points should be considered:

- **Detailed impact analysis**: Analyse the impact of dredging and disposal, and sand mining over the past decades, particularly the significant rise in bed levels in the intertidal areas at the middle and eastern parts of the estuary from 1965 to 1970.
- **Address model uncertainties**: Predictions under climate change and SLR scenarios imply uncertainty in model outcomes. Future studies on SLR impact could apply different model methodologies (ASMITA/ESTMORF, Delft3D Hybrid), to gain trust in model outcomes and explore uncertainty ranges.
- **Develop a conceptual framework**: Create a conceptual framework addressing the potential and limitations of human interventions on short-term (~decades) and long-term (~century) intertidal area evolution. This framework would benefit from closer insight into perspectives for action and management in light of climate change.

6 References

De Vet, P. L. M., Van Prooijen, B. C., & Wang, Z. B. (2017). The differences in morphological development between the intertidal flats of the Eastern and Western Scheldt. Geomorphology, 281, 31–42. https://doi.org/10.1016/j.geomorph.2016.12.031

Elias, E. P. L., Van Der Spek, A. J. F., Wang, Z. B., Cleveringa, J., Jeuken, C. J. L., Taal, M., & Van Der Werf, J. J. (2023). Large-scale morphological changes and sediment budget of the Western Scheldt estuary 1955–2020: The impact of large-scale sediment management. Netherlands Journal of Geosciences, 102, e12. https://doi.org/10.1017/njg.2023.11

Elmilady, H., Van Der Wegen, M., Roelvink, D., & Van Der Spek, A. (2020). Morphodynamic Evolution of a Fringing Sandy Shoal: From Tidal Levees to Sea Level Rise. Journal of Geophysical Research: Earth Surface, 125(6), e2019JF005397. https://doi.org/10.1029/2019JF005397

Elmilady, H., Van Der Wegen, M., Roelvink, D., & Van Der Spek, A. (2022). Modelling the Morphodynamic Response of Estuarine Intertidal Shoals to Sea-Level Rise. Journal of Geophysical Research: Earth Surface, 127(1), e2021JF006152. https://doi.org/10.1029/2021JF006152

Jeuken, MCJL., Wang, ZB., Keiller, D., Townend, I., & Liek, GA. (2003). Morphological response of estuaries to nodal tide variation. In Irtces, & Zihe (Eds.), *Proceedings of the international conference on Estuaries and Coasts* (pp. 166-173). IRTCES.

Marijs, K., & Parée, E. (2004, May). Nauwkeurigheid vaklodingen Westerschelde en -monding: "de praktijk" (tech. rep. No. ZLMD-04.N.004). Rijkswaterstaat. Vlissingen.

Paternotte, L., 2024. Model validation for the evolution of intertidal areas in the Western Scheldt. University of Twente, Enschede, The Netherlands.

Röbke, B. R., Elmilady, H., Van Der Wegen, M., & Taal, M. (2020, December). The long term morphological response to sea level rise and different sediment strategies in the Western Scheldt estuary (The Netherlands) (tech. rep.). Deltares. Delft.

Schepers, L., Maris, T., Meire, P., & Temmerman, S. (2018). The Scheldt Estuary: An Overview of the Morphodynamics of Intertidal Areas. In A. Demoulin (Ed.), Landscapes and Landforms of Belgium and Luxembourg (pp. 281–296). Springer International Publishing. https://doi.org/10.1007/978-3-319-58239-9_17

Storm, C., Bollebakker, P., De Jong, J., & Mol, G. (1993, February). Nauwkeurigheid zandbalans Westerschelde 1965-1990 en aanbevelingen er optimalisatie (tech. rep.No. RIKZ-94.008). Rijkswaterstaat.

Wang, Z. B., & Van Der Spek, A. (2015, July). Importance of mud for morphological response of tidal basins to sea-level rise. *The Proceedings of the Coastal Sediments 2015*. Coastal Sediments 2015, San Diego, USA. https://doi.org/10.1142/9789814689977_0208

Wang, Z. B., Elias, E. P. L., Van Der Spek, A. J. F., & Lodder, Q. J. (2018). Sediment budget and morphological development of the Dutch Wadden Sea: Impact of accelerated sea-level rise and subsidence until 2100. Netherlands Journal of Geosciences, 97(3), 183–214. https://doi.org/10.1017/njg.2018.8

Zheng, J., Elmilady, H., Röbke, B. R., Taal, M., Wang, Z. B., van Prooijen, B. C., ... & Van der Wegen, M. (2021). The impact of wind-waves and sea level rise on the morphodynamics of a sandy estuarine shoal. *Earth Surface Processes and Landforms*, *46*(15), 3045-3062.

A Morphological features of the Western Scheldt

Figure A. 1 presents the main morphological features of the Western Scheldt with their respective names. Figure taken from Elias et al. (2023).

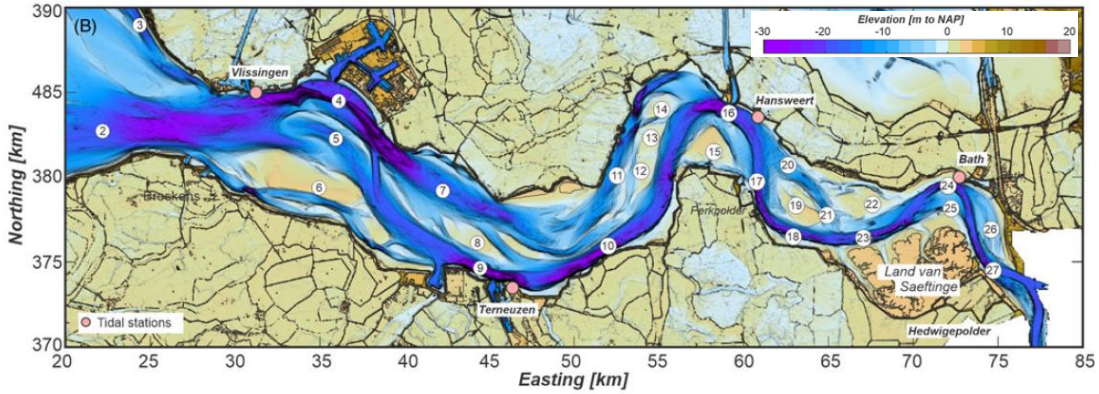

1. Vlakte van de Raan	6. Hooge Platen	12. Rug van Baarland	17. Zuidergat	23. Overloop van Valkenisse
2. Wielingen	7. Everingen	13. Plaat van Ossenisse West	18. Bocht v. Walsoorden	24. Nauw van Bath
3. Oostgat	8. Middelplaat	14. Molenplaat	19. Plaat van Walsoorden	25. Plaat van Saeftinge
4. Honte	9. Pas van Terneuzen	15. Plaat van Ossenisse	20. Schaar van Waarde	26. Ballastplaat
5. Spijkerplaat	10. Gat van Ossenisse	16. Put van Hansweert	21. Schaar van Valkenisse	27. Pas van Rilland
	11. Middelgat		22. Platen van Valkenisse	

Figure A. 1. Main channels and shoals of the Western Scheldt estuary. It is based on bathymetry data collected in 2021. Depths in m relative to Dutch ordnance datum NAP (Normaal Amsterdams Peil), which is about present-day mean sea level. Source: Elias et al. (2023)

B Additional information related to the model hindcasts

B.1 Observations in Vaklodingen dataset

The Vaklodingen dataset was visually inspected with QGIS. The intention was to find an area where measurements were present for all the analysed years (1965-2010). From this inspection, the following observations were made:

- From 1960 to 1995, measurements were carried out for half the estuary, alternating between the eastern and western parts. For some years, data was also missing in small portions of the Western Scheldt.
- From 1960 until 2010 the same region was measured, from Vlissingen to the Dutch-Belgian Border of the Western Scheldt. In recent years the mouth area and part of the Western Scheldt, east of Land van Saeftinghe were also included in the data.
- Because of land reclamation and managed realignment (Dutch: ontpoldering), some areas were intertidal in the past, but now they are on the landward side of the embankments, and vice versa. Until 2010, the changes were not considered in the measurements (see B.1, for an example). It is after 2010, that the shoreline has been included more accurately.

To form complete bathymetries to compare with the model hindcasts, it was decided to combine data from consecutive years (see

Table 6.1). In addition to this, a polygon was drawn using QGIS, where areas that were not present for all years (e.g., because of managed realignment) and/or that contained errors were excluded. This polygon can be observed in Figure 2-2, and captures the total study area of the Western Scheldt.

Table 6.1. Overview of the choices made to define complete bathymetries to compare with model hindcasts

Representative year	Description
1965	Combined data of 1965 and 1966
1970	Combined data of 1970 and 1971
1975	Combined data of 1975 and 1976
1985	Not included. There was missing data between Vlissingen-Oost and Terneuzen in the period 1983-1987.
1995	1996 was the actual year used since it provided a complete dataset.

The Vaklodingen dataset has stochastic (random) and systematic errors (bias) in determining the bed levels. Because the stochastic errors are in both negative and positive directions, they are negligible if a relatively large area is considered (Marijs and Parée, 2004). The systematic error of the Vaklodingen for intertidal areas has been determined as -0.20 m (Storm et al., 1993). This means that at least until 1990, the last year considered in an accuracy study carried out by Storm et al. (1993), the bed levels of intertidal areas have been measured lower than the actual values. De Vet et al. (2017) suggests that with the inclusion of LiDAR technology from 2001 onwards, the accuracy of the Vaklodingen has improved and errors are in the order of 10 cm.

In section Figure 2-2it was mentioned that up until 2010, the same area of the Western Scheldt was measured regardless of managed realignment that was carried out. Figure B. 1 presents an example of this situation, where Bathse Schor, a former intertidal area in the eastern part of the estuary was reclaimed in the early 70s. The left panel of this figure shows a topographic map of the time when this area was still intertidal. The right panel presents Vaklodingen data for 2010, where it can be observed that this region was still surveyed (notice the yellow line of the dike and misalignment with the satellite image).

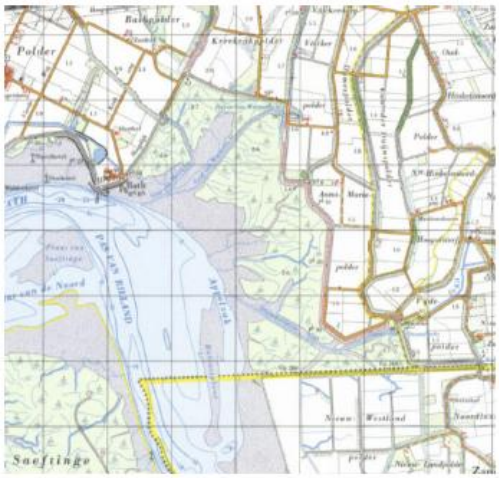

(a) Topographic map (ca. 1970, source: topotijdreis.nl).

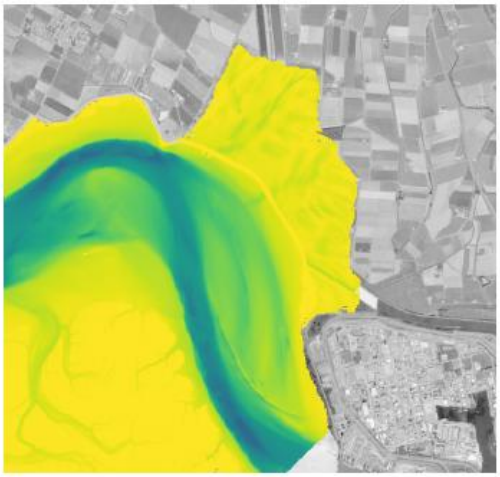

(b) Vaklodingen data 2010.

Figure B. 1. Bathse schor area in a) 1970, when it was still an intertidal area, and b) 2010, when it has been reclaimed for several years already, but still forms part of the Vaklodingen dataset. Source: Paternotte (2024)

B.2 Effect of interpolation of the Vaklodingen to the model grid and step size used to compute hypsometric curves

As it was mentioned in the main text, the Vaklodingen dataset consists of grids of 20x20 m. On the other hand, the grid of the Delft3D-Scheldt-SLR model has a representative grid in the Western Scheldt of 200 m by 100 m. Therefore, the bathymetric data has a higher resolution. Nevertheless, to ease the postprocessing of the measured bed levels, it was decided to interpolate the Vaklodingen dataset in the grid of the Delft3D-Scheldt-SLR model. A sensitivity analysis was performed to determine the impact of such interpolation on the results. It was found that, on average, the intertidal area decreased by 3% after the interpolation; and that the larger cell sizes of the model grid, led to less smooth curves (see Figure B. 2). It is considered that these findings have a limited impact in the conclusions with respect to the validation of the model.

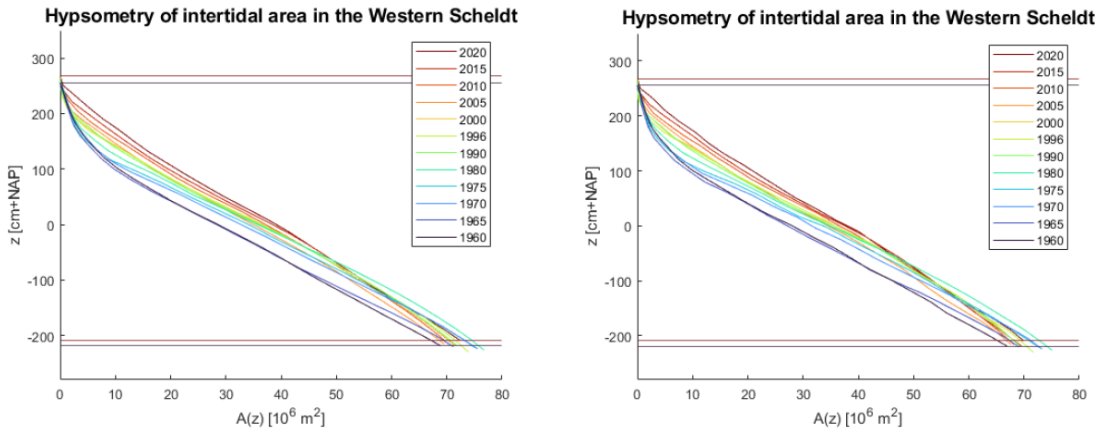

Figure B. 2. Comparison of the hypsometric curves based on the Vaklodingen when: a) using its original grid, b) when using the grid of the Delft3D-Scheldt-SLR model.

B.3 Effect of implementation of dredging and disposal in the model

One of the major limitations of the Delft3D-Scheldt-SLR model is the way that dredging and disposal is carried out. When dredging and disposal is activated, then it all happens in one single computational timestep instead of on a prolonged period of time as it happens in reality. This led to abrupt changes in the bed levels that later would take quite some time to smooth out. Two examples can be observed in Figure B. 3, where sediment was deposited in the main channel, at the east for the upper panel, and at the middle of the estuary for the lower panel.

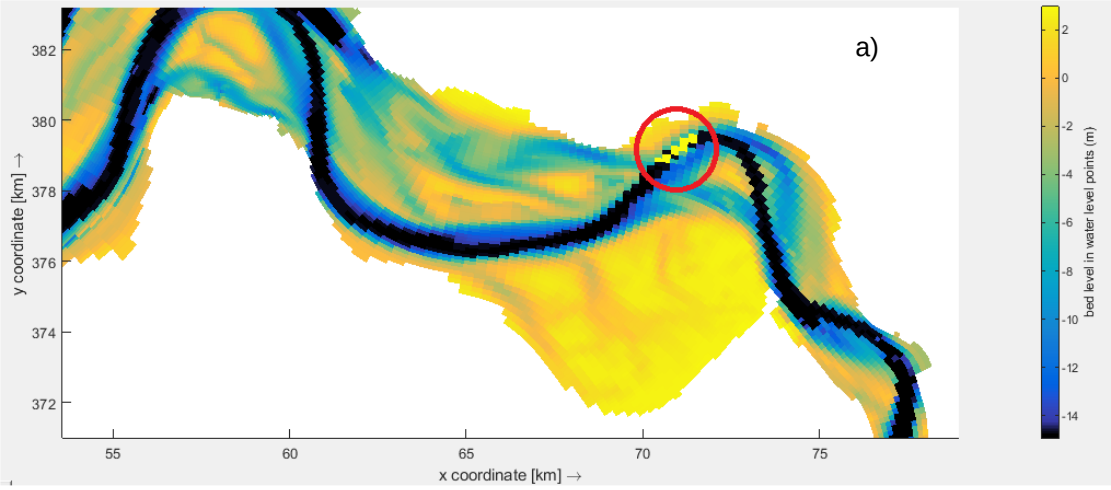

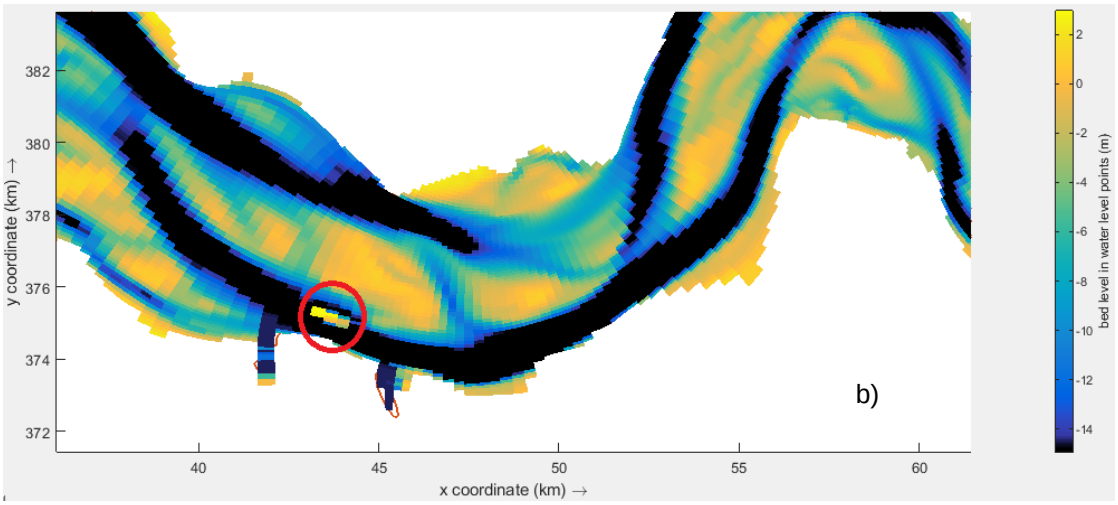

Figure B. 3. Bed levels subtracted from the no-wave hindcast around 1975 (upper panel) and 1965 (lower panel). The red circles enclose locations where sediment was disposed.

B.4 Effect of the nodal-cycle in the computation of water levels

When the tidal nodal cycle is taken into account in the definitions of the 50% highest high water and 50% lowest low water, then differences in the tidal range of 20 and 40 cm can be found at Vlissingen and Bath (Figure B. 4). However, if this variability is taken into consideration for the computation of the hypsometric curves, not major effect can be found in their trends (

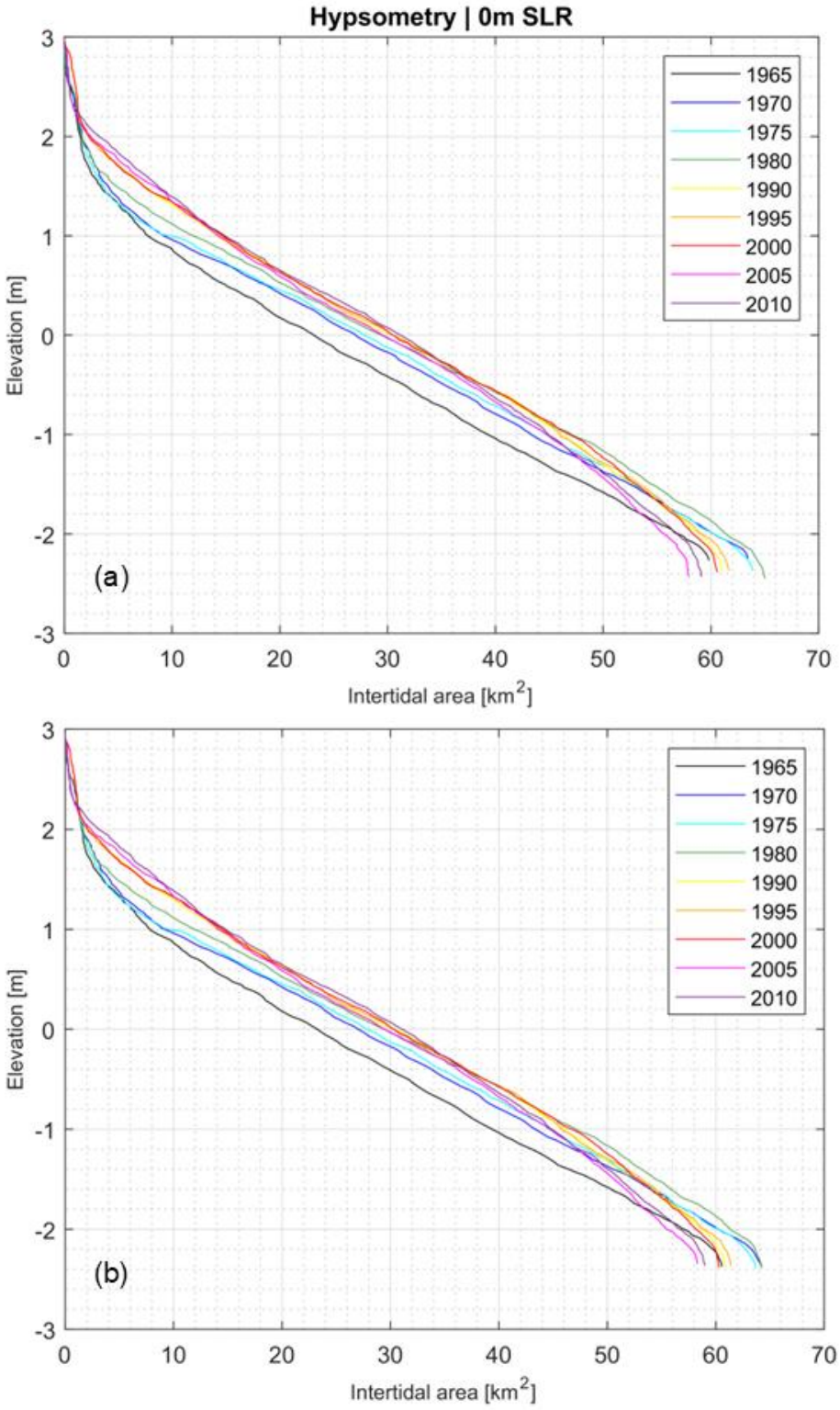

Figure B. 5).

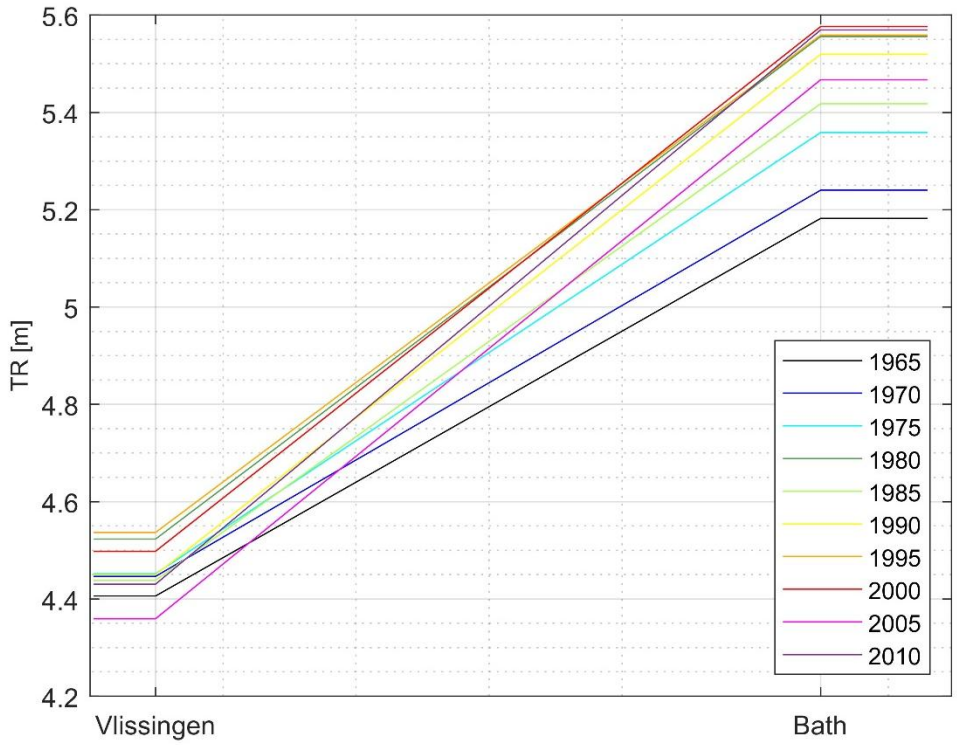

Figure B. 4. Tidal range based on the average 50% highest high and lowest low water levels from the period 1955 to 2023 at Vlissingen and Bath, for all the analysed years.

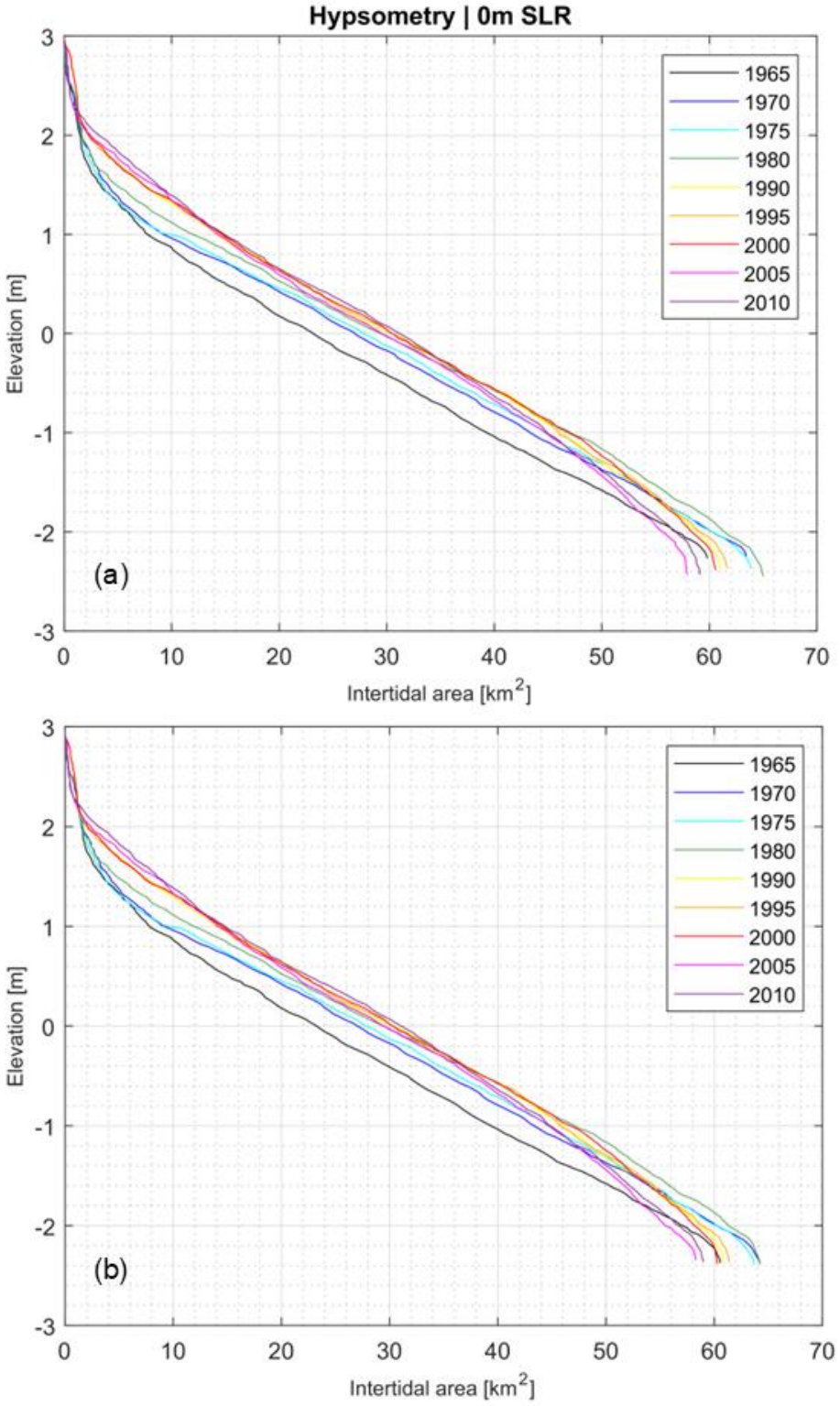

Figure B. 5. Hypsometric curves based on the Vaklodingen computed with the inclusion (a) and exclusion (b) of the tidal nodal cycle.

Deltares is an independent institute for applied research in the field of water and subsurface. Throughout the world, we work on smart solutions for people, environment and society.

Deltares

www.deltares.nl